DOE/PC/94222-10

TUNABLE COMPOSITE MEMBRANES FOR GAS SEPARATIONS

Quarterly Progress Report

April 1997 - June 1997

J. P. Ferraris, K. J. Balkus, Jr. and I. H. Musselman

July 1997

PREPARED FOR THE U. S. DEPARTMENT OF ENERGY
UNDER AWARD NUMBER DE-FG22-94PC94222

Department of Chemistry
The University of Texas (Dallas)
P. O. Box 830688
Richardson, Texas 75083-0688

Disclaimer:

This report was prepared as an account of work sponsored by an agency of the United States Government. Neither the United States Government nor any agency thereof, nor any of their employees, makes any warrant, express or implied, or assumes any legal liability or responsibility for the accuracy, completeness, or usefulness of any information, apparatus, product, or process disclosed, or represents that its use would not infringe privately owned rights. Reference herein to any specific commercial product, process, or service by trade name, trademark, manufacturer, or otherwise does not necessarily constitute or imply its endorsement, recommendation, or favoring by the United States Government or any agency thereof. The views and opinions of the authors expressed herein do not necessarily state or reflect those of the United States Government or any agency thereof.

Abstract:

Solution cast membranes of poly(3-dodecylthiophene) (PDDT) were studied for the room temperature separation of N_2, O_2, and CO_2. A procedure for fabricating reproducible, smooth, uniformly thick (~35-μm), defect-free membranes was established. Permeability values were measured for as-cast PDDT membranes (P_{N_2} = 9.4, P_{O_2} = 20.2, P_{CO_2} = 88.2 Barrers) and selectivity values were calculated (α_{O_2/N_2} = 2.2, α_{CO_2/N_2} = 9.4). Chemically induced doping (~23%) with $SbCl_5$ resulted in a decrease in permeability (P_{N_2} = 3.5, P_{O_2} = 10.5, P_{CO_2} = 48.5 Barrers) and a corresponding increase in permselectivity (α_{O_2/N_2} = 3.0, α_{CO_2/N_2} = 14.0). Membrane undoping with hydrazine partially reversed these trends (P_{N_2} = 5.4, P_{O_2} = 15.1, P_{CO_2} = 62.9 Barrers, α_{O_2/N_2} = 2.8, α_{CO_2/N_2} = 11.6). The chemical compositions of as-cast, doped, and undoped PDDT membranes were determined using elemental analysis and energy dispersive x-ray spectrometry. Membrane microstructure was investigated by optical microscopy, TappingMode™ atomic force microscopy and scanning electron microscopy. The composition and microscopy results were correlated with changes in gas-transport properties. Two papers were presented at the Meeting of the North American Membranes Society, (June 2-4, 1997, Baltimore, MD).

Table of Contents

Executive Summary:

During this past quarter of project DE-FG22-94PC94222, continued significant progress was made in the synthesis and characterization of conducting polymer composite membranes for gas separations. Highlights from this funding period include:

- The permeability and permselectivity of as-cast, chemically doped and undoped poly(3-dodecylthiophene) membranes towards N_2 , O_2 and CO_2 were measured and correlated with microstructure.

- Paper entitled "Poly(3-alkylthiophene)/Molecular Sieve Composite Membranes for Gas Separations", D. Smithhisler, K. Balkus, Jr., J. Ferraris, I. Musselman and S. Riley, presented at the North American Membranes Society meeting (Baltimore, MD, June 2-4, 1997) **Paper was awarded a Student Travel Grant from NAMS**

- Paper entitled "Poly(3-alkylthiophene) Membranes for Gas Separations" , I. H. Musselman, L. Li, L. Washmon, S. J. Riley, J. P. Ferraris, K. J. Balkus, Jr., presented at the North American Membranes Society meeting (Baltimore, MD, June 2-4, 1997)

Introduction:

The use of membrane technology for gas separations offers significant thermodynamic and economic advantages over distillation processes. Target separations of importance to the coal and energy fields include N_2/O_2 , H_2S/syngas and CO_2/CH_4. Current strategies for improving these separations are largely directed towards processable polymers with thin (<500 Å) skins. Unfortunately most polymeric materials that provide commercially viable permeation rates exhibit poor selectivities and *vice versa* and there are inherent limitations in gas permeability/permselectivity for pure polymers. Our strategy relies on modification of composite membranes, preferably *in situ,* to enhance the permselectivity while maintaining acceptable permeabilities. The composites consist of electroactive polymers (which can be switched from rubbery to glassy), filled with selective absorbents (zeolites) which are impregnated with metals or catalysts to effect facilitated transport. The project is multifaceted and involves the efforts of a polymer synthesis group, a microporous materials group, a microscopy group and a permeability measurements group, all working in concert. This report summarizes the results of our efforts for last quarter.

Experimental

Polymer synthesis and characterization

Random poly(3-dodecylthiophene) (PDDT) was synthesized using the method described by Tamao et al. Molecular weights of the PDDT (Mw = 249,100, Mn = 96,300) were determined by gel permeation chromatography (GPC) ($CHCl_3$, 5 mg/ml) using a Viscotek Model LR 40 calibrated with polystyrene standards. Ultraviolet/visible spectroscopy (Hitachi U2000) of PDDT in chloroform revealed a λ_{max} of 433 nm confirming the regiorandom backbone coupling of the polythiophene.

Membrane fabrication

Small insoluble particulate matter was removed from the polymer by stirring the PDDT at room temperature overnight in HPLC grade chloroform followed by sequential filtration using a stainless steel syringe holder containing Millipore filters of decreasing pore size (8.0, 5.0, 3.0, 1.2 and 0.45 μm). The solution was then evaporated to dryness and the red polymer was transferred to an evaporation dish and placed in the dark at room temperature to evaporate the residual solvent. The purified PDDT was stored under nitrogen in the dark to minimize chemical and photooxidation.

For casting membranes, a 10% w/w solution of the dry, filtered polymer in tetrachloroethylene (99%) was prepared. The solution was stirred overnight and sonicated for 40 min to ensure complete dissolution. In a laminar flow hood (PureAire), membranes were cast on glass using an AccuLab Jr.™ Drawdown casting table equipped with a wire wound rod (AccuLab Jr.™ 48-76). A 0.85 mL aliquot of the polymer solution was transferred by pipet onto the clean glass substrate and then spread using the casting rod. The membrane was partially covered to slow solvent evaporation and to minimize photooxidation. Upon drying, a deep green membrane approximately 35 μm thick was formed. The membrane appeared translucent red by transmission.

Polymer membranes were annealed in a vacuum oven for 3 h at 393 K and subsequently allowed to cool under vacuum. Annealing serves to drive off residual solvent and to promote viscous flow, thus minimizing holes and defects in the membrane.

Establishing redox protocols

SEM/EDS was particularly valuable in establishing experimental procedures to oxidize and reduce PDDT membranes. SEM images were acquired from cross sections of as-cast, doped and undoped membranes to reveal their internal microstructures. When establishing the reduction protocol, a sandwich structure was initially observed for a membrane that was immersed in 10% hydrazine for 0.5 h. The inner (~20 μm) and outer

(~10 µm) microstructures of this sandwich resembled those of the as-cast and doped membranes, respectively. High and low antimony-to-sulfur (Sb/S) ratios were found to correlate with the outer and inner microstructures, respectively. Subsequent immersion of a doped membrane in 10% hydrazine for 3 h resulted in the formation of a uniform internal microstructure similar to that observed for the as-cast membrane for which the Sb/S ratio was smaller and constant throughout its thickness. These results suggest that the Sb anion partially diffused out of the membrane during reduction. Reduction for 2 h in a 15% aqueous hydrazine solution, as implemented for the combined permeability/microscopy studies, yielded similar results.

Membrane doping/undoping

Membrane doping was accomplished using two methods. In the first method, a membrane was oxidized for 45 min under N_2 in a Vacuum Atmosphere Co. glove box using a 3% w/w solution of antimony pentachloride ($SbCl_5$) in dry acetonitrile. The p-doped membrane was rinsed with dry acetonitrile and the rinse solvent was tested with ferrocene to insure complete removal of residual oxidant. In the second method, the oxidation process was conducted in a glove bag (I^2R, Inc.) under N_2. In the glove bag, a membrane was immersed for 3 h in a 15% w/w solution of $SbCl_5$ in dry acetonitrile. The doped membrane was then rinsed and tested as described above. The p-doped membranes were slightly brittle and dark blue in color. PDDT membranes were chemically undoped by immersing them for 2 h in a 15% w/w aqueous solution of hydrazine followed by rinsing with NANOpure™ (Barnstead) water. The undoped membrane was flexible and red in color.

Membrane characterization

Membrane morphology

Membrane surface morphology was investigated using optical microscopy (OM) (Wild-Leitz Ergolux Microscope), scanning electron microscopy (SEM) (Phillips XL 30)

and TappingMode™ atomic force microscopy (TMAFM) (Nanoscope III Multimode Scanning Probe Microscope, Digital Instruments, Inc.). The internal microstructure of the membrane was revealed through SEM of sample cross sections. Samples for OM and AFM were secured to steel pucks (Digital Instruments, Inc.) with double-stick conductive carbon tabs (Ted Pella). Samples for SEM surface imaging were attached similarly to aluminum SEM stubs (Ted Pella). Membrane cross sections, prepared by freeze fracture [16], were mounted in a cross section holder. All SEM samples were carbon-coated (Denton Vacuum DESK II Cold Sputter/Etch Unit with Carbon Evaporation Accessory) to eliminate sample charging. The OM reticle was calibrated (1.6 μm/div) at 1000x using a stage micrometer (Ronchi). The AFM J scanner was calibrated using a 10 μm pitch grating with a step height of 180 nm (Digital Instruments, Inc.). Values of root-mean-square roughness, R_{rms}, i.e. the standard deviation of the height values, were determined for each TMAFM image.

Membrane chemistry

Membrane composition was determined by elemental analysis (Galbraith Laboratories, Inc.), scanning electron microscopy/energy dispersive x-ray spectrometry (SEM/EDS) (Phillips XL 30, EDAX PV9800) and x-ray photoelectron spectroscopy (Kratos AXIS HS, Al Kα x-ray source, 40 eV pass energy, 90° take-off angle). Uniformity of doping/undoping across the thickness of the membrane cross section was evaluated using SEM/EDS by measuring the Sb Lα / S Kα intensity ratio for adjacent areas.

Membrane permeability and selectivity

A custom built permeameter incorporating upstream and downstream manometers to measure gas pressure and flux, was operated using LabView software. Each membrane was placed on an aluminum support bearing a bronze frit in a stainless steel permeation cell. The rate of gas transport (N_2, O_2, CO_2) across the membrane was investigated in a

thermostated environment (308 - 310 °K) using single-gas-permeation measurements. Following evacuation of the permeameter, the membrane was degassed in vacuum until a downstream steady-state leak rate of <20 mtorr/hour was obtained. Using an upstream pressure, P_1, of 110 cmHg, four 15 minute permeability experiments per test gas were conducted by measuring the downstream pressure-time transient, $\Delta P_2/\Delta t$. Each experiment was followed by a 1 hour cell evacuation for membrane degassing. The permeability coefficient, *P*, was determined from three experiments for each test gas. Selectivity coefficients, α, were obtained from the ratio of permeability coefficients for two gases.

Membrane thickness

The knowledge of membrane thickness is critical to calculating accurate values of gas permeability. Confidence in membrane thickness uniformity for the region of membrane exposed to gas in the permeameter is also important. Optical microscopy proved to be an accurate and reliable method for both determinations. Using a calibrated Wild-Leitz Ergolux Microscope thickness measurements were obtained from polymer membrane cross sections prepared using conventional freeze fracture techniques. The microscope calibration was verified by measuring the thickness of Mylar 48A (12.19 µm). The error associated with the thickness measurement of the Mylar standard was less than 12%.

Results and Discussion

In comparison with as-cast membranes, chemical oxidation results in a decrease in permeability and an increase in permselectivity. These trends are partially reversed with chemical reduction. Elemental analysis and microscopy/spectroscopy methods are used to characterize membrane chemistry and microstructure. For as-cast PDDT membranes, optical microscopy (OM) reveals a smooth and featureless surface on the 200 µm scale.

OM and scanning electron microscopy (SEM) demonstrate that these membranes are dense and uniformly thick, an important quality for the accurate measure of gas permeability. By TappingMode™ atomic force microscopy (TMAFM), the as-cast membranes appear extremely smooth, exhibiting a root-mean-square surface roughness, R_{rms}, of approximately 3 nm over a 100 μm^2 area. With chemical doping (R_{rms} = 21 nm) and undoping (R_{rms} = 110 nm), the PDDT surface becomes more rough. The internal membrane microstructure, which appears more coarse following oxidation, partially returns to its dense structure following undoping. Cross-sections for as-cast, doped, partially undoped and completely undoped PDDT membranes are shown in Figure 1.

Permeability studies of PDDT were conducted sequentially for the test gases N_2, O_2 and CO_2. The average permeabilities (P_{N_2}, P_{O_2}, P_{CO_2}) for each of 6 as-cast membranes are reported in Table 1 as the mean values for 3 successive exposures to each test gas. A rubbery polymer at room temperature (T_g = 253 °K) , PDDT exhibited characteristically high permeabilities (P_{N_2} = 9.4 Barrers, P_{O_2} = 20.2 Barrers, P_{CO_2} = 88.2 Barrers) and low permselectivities (α_{O_2/N_2} = 2.2, α_{CO_2/N_2} = 9.4) (Table 1, Figure 2). The values of permeability and permselectivity are reproducible and the observed measurement error (<10%) falls within the nonuniformity of PDDT membrane thicknesses (<11%). Permeability measurements obtained for a second batch of as-cast PDDT with a lower molecular weight (Mw = 139,000, Mn = 38,600) yielded similar results.

Permeability data are listed in Table 2 for 6 membranes oxidized for 45 min in a glove box using a 3% w/w solution of $SbCl_5$ in acetonitrile. Elemental analysis results revealed a 9% doping level for membranes oxidized in this manner. In comparison with the as-cast membranes, the permeability values for the test gases increased slightly with membrane oxidation (Table 2, Figure 2): P_{N_2} increased 13% to 10.6 Barrers, P_{O_2} increased 15% to 23.1 Barrers and P_{CO_2} increased 21% to 106.3 Barrers. There were no significant changes for the permselectivity values: α_{O_2/N_2} = 2.2, α_{CO_2/N_2} = 10.1. The errors in the

grand average values were ≤8% which again demonstrated that the permeability measurements were reproducible.

Permeability data is presented in Table 3 for 5 membranes oxidized for 3 h in a glove bag using a 15% w/w solution of $SbCl_5$ in acetonitrile. Elemental analysis results revealed a 23% doping level for membranes oxidized in this manner. Compared to the as-cast PDDT membranes (Figure 2), a decrease in gas permeabilities of more than 45% was observed: P_{N_2} = 3.5 Barrers, P_{O_2} = 10.5 Barrers and P_{CO_2} = 48.5 Barrers. This decrease in permeability was accompanied by an increase in permselectivity: α_{O_2/N_2} = 3.0, α_{CO_2/N_2} = 14.0.

The observed decrease in permeability and corresponding increase in permselectivity of PDDT with high levels of doping is caused by changes in diffusivity and solubility. After the polymer is oxidized, a more rigid conformation is adopted which curtails the rotational freedom of the polymer backbone and results in a decrease in the short and long range agitation motion of the polymer chains. The filling of the charge balancing anion also decreases the free volume. Solubility, which is dependent on gas-polymer interactions, increases with oxidation because the charges associated with the S and the charge balancing anions, introduced along the backbone upon doping, make the polymer more polar.

The extent to which diffusivity decreased and solubility increased with oxidation was largely dependent on the doping level. Membranes doped at a low level (~9%) exhibited a slight decrease in diffusivity but a relatively large increase in solubility resulting in a net increase in gas permeability (Table 2) as compared to as-cast PDDT membranes (Table 1). Since all the permeability values increased slightly (13%-21%), no significant change in permselectivity was observed. Membranes oxidized in 15% $SbCl_5$ for 3 h were more rigid and exhibited a higher level of doping (~23%). As a result, the diffusivity decreased to a larger extent than the solubility increased. Consequently, a significant decrease in permeability was observed (Table 3). These highly doped PDDT membranes also exhibited an increase in permselectivity suggesting that the rigid structure

acted like a “molecular sieve” that could discriminate among gas molecules of different sizes and shapes.

Five membranes oxidized in a 15% solution of $SbCl_5$ in acetonitrile for 3 h and then reduced in 15% aqueous hydrazine for 2 h were tested with the permeameter (Table 4, Figure 2). After this one doping/undoping cycle, the measured permeabilities (P_{N_2} = 5.4, P_{O_2} = 15.1, P_{CO_2} = 62.9) and permselectivities (α_{O_2/N_2} = 2.8, α_{CO_2/N_2} = 11.6) were between those of the as-cast and doped membranes. When the polymer was undoped, the restriction to free rotation in the polymer backbone of the doped polymer was removed thereby increasing diffusivity. However, EDS analysis showed that the Sb content was still high in the undoped polymer thereby limiting the available polymer free volume. Hence, the contribution of diffusivity to permeability for the undoped membrane never completely returned to that of the as-cast membrane. As a result of undoping, the “molecular sieve” effect decreased and permselectivities lower than those of the doped membranes were observed.

Conclusion

With the help of SEM/EDS, conditions (e.g. concentration, reaction time) were established for oxidizing (via $SbCl_5$) and reducing (via hydrazine) the membranes. Characterization of the surface and interior of the as-cast membranes by OM, TMAFM, and SEM revealed a smooth, dense, uniformly thick, defect-free microstructure which changed with oxidation and reduction. For the as-cast PDDT membranes, N_2, O_2 and CO_2 permeability coefficients were measured (N_2 = 9.4, O_2 = 20.2, CO_2 = 88.2) and O_2/N_2 and CO_2/N_2 selectivity coefficients were calculated (α_{O_2/N_2} = 2.2, α_{CO_2/N_2} = 9.4). Permeabilities and permselectivities were controlled through chemical redox. The doped polymer (~23%) was found to have decreased values of permeability (P_{N_2} = 3.5 Barrers,

P_{O_2} = 10.5 Barrers, P_{CO_2} = 48.5 Barrers) and increased values of permselectivity (α_{O_2/N_2} = 3.0, α_{CO_2/N_2} = 14.0). After one oxidation/reduction cycle, the permeability (P_{N_2} = 5.4, P_{O_2} = 15.1, P_{CO_2} = 62.9) and permselectivity (α_{O_2/N_2} = 2.8, α_{CO_2/N_2} = 11.6) values were between those of the as-cast and doped membranes.

Figure 1

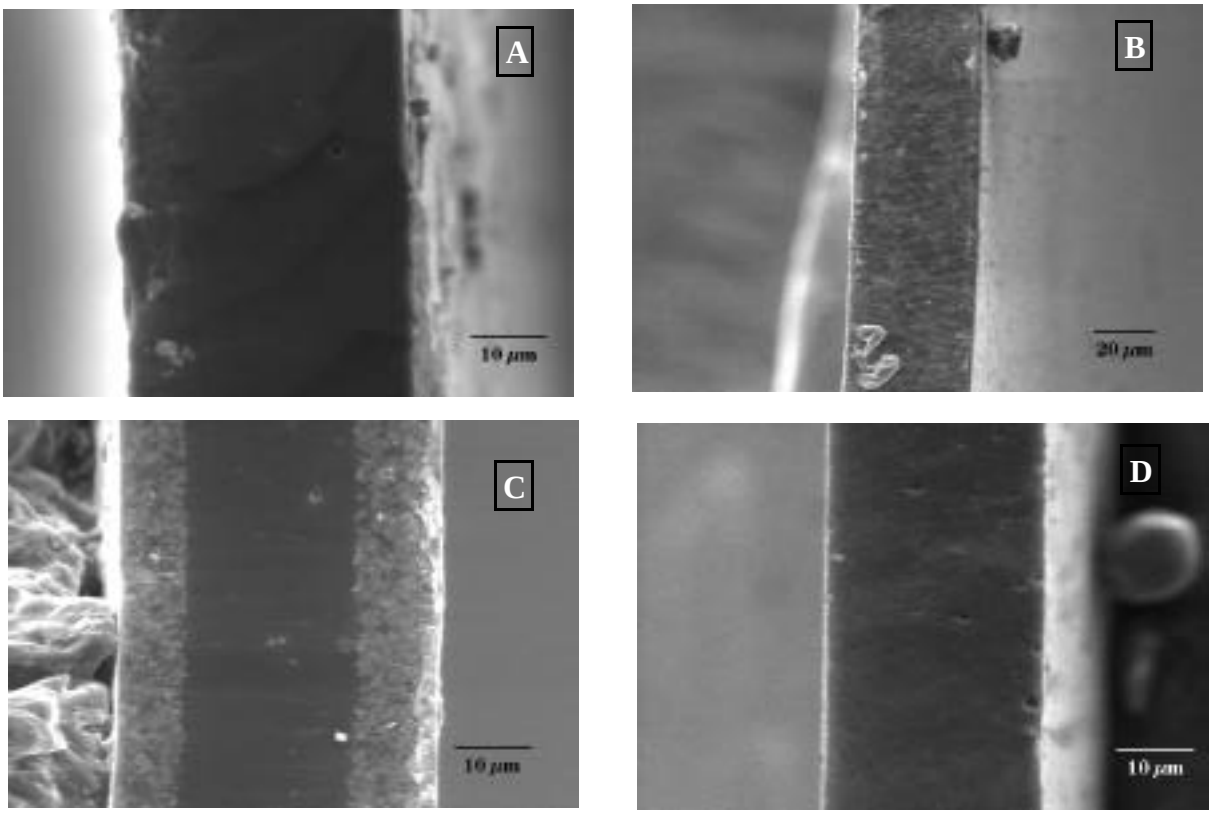

Figure 2

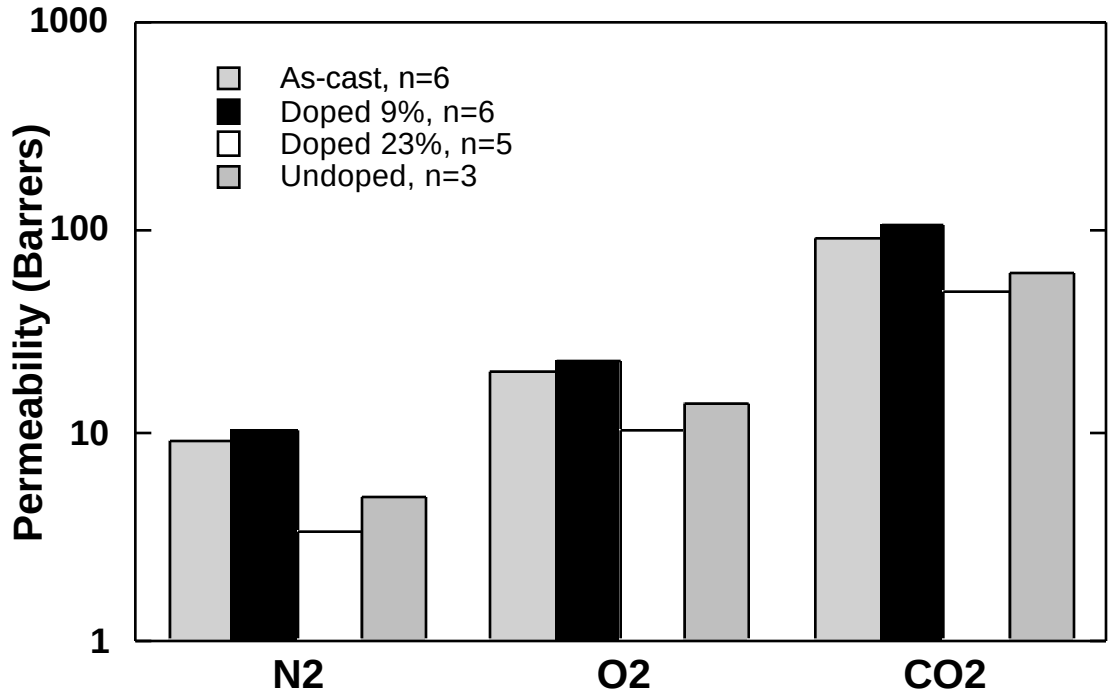
1000
100
10
1
Permeability (Barrers)
As-cast, n=6
Doped 9%, n=6
Doped 23%, n=5
Undoped, n=3
N2
O2
CO2

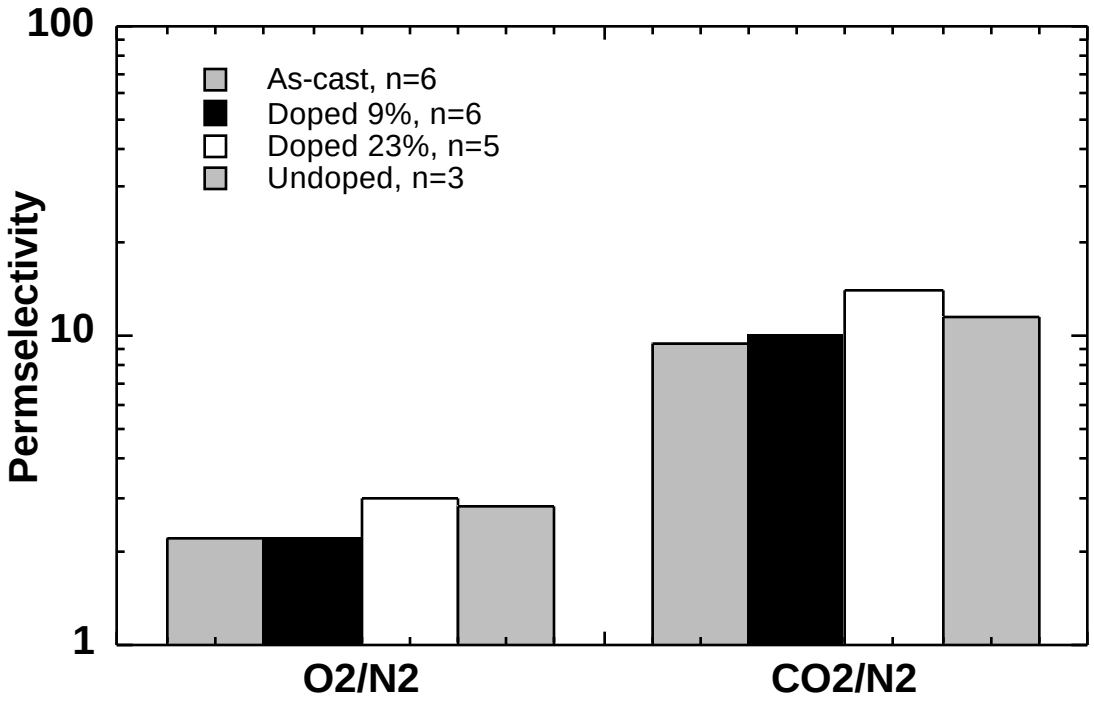
100
10
1
Permselectivity
As-cast, n=6
Doped 9%, n=6
Doped 23%, n=5
Undoped, n=3
O2/N2
CO2/N2

Table 1: Permeability and Selectivity Values for As-Cast PDDT Membranes

Mw = 249,100; Mn = 96,300

Membrane	P N_2	P O_2	P CO_2	a O_2/N_2	a CO_2/N_2
1	9.4 ± 0.2	21.8 ± 0.4	93.6 ± 0.2	2.3 ± 0.1	10.0 ± 0.2
2	8.7 ± 0.1	22.1 ± 0.4	98.0 ± 0.4	2.5 ±0.1	11.2 ± 0.1
3	10.1 ± 0.5	19.0 ± 0.4	84.0 ± 0.4	1.9 ± 0.1	8.3 ± 0.4
4	7.8 ± 0.2	19.0 ± 0.5	82.8 ± 0.0	2.4 ± 0.1	10.6 ± 0.3
5	10.2 ± 0.5	19.5 ± 0.1	83.0 ± 0.6	1.9 ± 0.1	8.1 ± 0.4
6	10.3 ± 0.4	20.0 ± 0.2	87.6 ± 0.6	1.9 ± 0.1	8.5 ± 0.3
Grand Avg.	**9.4 ± 0.9 (10%)**	**20.2 ± 0.9 (4%)**	**88.2 ± 1.0 (1%)**	**2.2 ± 0.2 (9%)**	**9.4 ± 0.7 (7%)**

Permeability coefficients in Barrers = 10^{-10} cm^3 (STM) cm/ cm^2 s cmHg.

Table 2: Permeability and Selectivity Values for Doped (~9%) PDDT Membranes

Mw = 249,100; Mn = 96,300

Membrane	P N_2	P O_2	P CO_2	a O_2/N_2	a CO_2/N_2
1	10.1 ± 0.1	23.6 ± 0.2	109.1 ± 0.7	2.3 ± 0.0	10.8 ± 0.1
2	10.1 ± 0.1	23.8 ± 0.2	108.8 ± 0.5	2.4 ± 0.0	10.8 ± 0.1
3	12.0 ± 0.4	22.6 ± 0.2	102.0 ± 0.8	1.9 ± 0.1	8.5 ± 0.3
4	10.3 ± 0.2	21.5 ± 0.2	100.2 ± 0.7	2.1 ± 0.0	9.7 ± 0.2
5	10.8 ± 0.2	24.5 ± 0.6	113.0 ± 0.8	2.3 ± 0.1	10.5 ± 0.2
6	10.0 ± 0.2	22.8 ± 0.5	104.6 ± 1.7	2.3 ± 0.1	10.5 ± 0.3
Grand Avg.	**10.6 ± 0.5 (5%)**	**23.1 ± 0.9 (4%)**	**106.3 ± 2.3 (2%)**	**2.2 ± 0.2 (8%)**	**10.1 ± 0.5 (5%)**

Permeability coefficients in Barrers = 10^{-10} cm^3 (STM) cm/ cm^2 s cmHg.

Table 3: Permeability and Selectivity Values for Doped (~23%) PDDT Membranes

Mw = 249,100; Mn = 96,300

Membrane #	P N_2	P O_2	P CO_2	a O_2/N_2	a CO_2/N_2
1	3.9 ± 0.0	11.6 ± 0.1	55.0 ± 0.9	2.9 ± 0.0	13.9 ± 0.2
2	2.6 ± 0.2	7.5 ± 0.0	36.3 ± 0.3	2.9 ± 0.2	13.9 ± 1.1
3	2.2 ± 0.1	7.2 ± 0.0	32.0 ± 0.4	3.3 ± 0.1	14.8 ± 0.7
4	4.2 ± 0.0	12.4 ± 0.0	57.3 ± 0.8	3.0 ± 0.0	13.7 ± 0.2
5	4.4 ± 0.1	13.6 ± 0.1	62.0 ± 1.3	3.1 ± 0.1	14.0 ± 0.4
Grand Avg.	**3.5 ± 0.2 (6%)**	**10.5 ± 0.1 (1%)**	**48.5 ± 1.8 (4%)**	**3.0 ± 0.2 (7%)**	**14.0 ± 1.4 (10%)**

Permeability coefficients in Barrers = 10^{-10} cm^3 (STM) cm/ cm^2 s cmHg.

Table 4: Permeability and Selectivity Values for Undoped PDDT Membranes

Mw = 249,100; Mn = 96,300

Membrane	P N_2	P O_2	P CO_2	a O_2/N_2	a CO_2/N_2
1	4.6 ± 0.1	12.7 ± 0.1	54.0 ± 0.7	2.8 ± 0.0	11.8 ± 0.2
2	5.6 ± 0.1	15.6 ± 0.1	64.5 ± 0.8	2.8 ± 0.1	11.5 ± 0.2
3	6.0 ± 0.1	16.9 ± 0.1	70.1 ± 1.6	2.8 ± 0.0	11.6 ± 0.3
Grand Avg.	**5.4 ± 0.2 (4%)**	**15.1 ± 0.2 (1%)**	**62.9 ± 1.9 (3%)**	**2.8 ± 0.1 (4%)**	**11.6 ± 0.4 (3%)**

Permeability coefficients in Barrers = 10^{-10} cm^3 (STM) cm/ cm^2 s cmHg.